

DESIGN AND ANALYSIS OF STANDALONE PV SYSTEM

**A thesis submitted in partial fulfilment of the requirements for the award of
the degree of**

Bachelor of Technology in “Electrical Engineering”

By

Chinmay Garanayak (111EE0033)

Bipin Bihari Behera (111EE0195)

Under the supervision of

Prof. Somnath Maity



**Department of Electrical Engineering
National Institute Of Technology, Rourkela
Rourkela – 769008, Odisha**



DEPARTMENT OF ELECTRICAL ENGINEERING
NATIONAL INSTITUTE OF TECHNOLOGY, ROURKELA

CERTIFICATE

This is to certify that the thesis entitled “**Design and analysis of Standalone PV System**”, submitted by **Chinmay Garanayak**, Roll no. **111EE0033** and **Bipin Bihari Behera**, Roll no. **111EE0195**, in partial fulfilment of the requirements for the award of **Bachelor of Technology in Electrical Engineering** at **National Institute of Technology, Rourkela**. A bonafied record of research work carried out by them under my supervision and guidance. The candidates have fulfilled all the prescribed requirements. To the best of my knowledge and belief, the reports and results embodied in this thesis have not been submitted elsewhere for a degree or diploma. In my opinion, the thesis is of the required standard for the award of a degree in Bachelor of Technology in Electrical Engineering.

Place: Rourkela

Date: 11 May 2015

Prof. Somnath Maity

Dept. of Electrical Engineering

NIT, Rourkela

ACKNOWLEDGEMENTS

We would like to express our indebtedness and deepest gratitude to our supervisor **Prof. Somnath Maity**, Dept. of electrical Engineering, NIT Rourkela, for his guidance, motivations, immense knowledge and extended confidence at every step due to which it is possible for us to complete the work in the stipulated time. We also thank him for his valuable suggestions and insightful comments which inspired us to explore more information regarding the project. We also express our indebtedness to all Faculty and staff of Dept. of Electrical Engineering for their support by establishing a working environment. Finally we would also like to acknowledge our friends for their suggestions and cooperation at various steps while completing this thesis.

Chinmay Garanayak

Bipin Bihari Behera

Dept. of Electrical Engineering

NIT Rourkela

CONTENTS

Abstract	5
List of Figures	6
List of Tables	7
1. Introduction	8
2. Literature survey	9
3. PV System	11
3.1. Solar Energy	11
3.2. Photovoltaic cell	11
3.3. Working Principle	12
4. Maximum Power Point Tracking	14
4.1 MPPT Techniques	14
4.1.1. Control system with current or voltage reference	15
4.1.2. Incremental Conductance Method	15
4.1.3. Perturb and Observe Method	15
4.2 MPPT Algorithm	16
5. DC – DC Converter	17
5.1 Working Principle	17
5.2 Simulink model and results	18
6. Inverter	20
6.1 Modelling of output voltage controller	22
6.2 Compact form expression for the exact switched model	23
6.3 Transferring the model into small signal averaged model	23
6.4 Effect of variation of different parameters upon inverter	26
6.5 Inverter model and results	28
7. Simulink model of PV system	32
7.1 Results	32
8. H – Bridge Inverter IC	34
8.1 Features	34
8.2 Pin configuration	35
9. Conclusion	37
10. References	38

ABSTRACT

Most of the energy sources originate from tried and conventional sources like fossil fuels, for example, coal, natural gasses and crude oil. Then comes the hydro power systems. These powers are frequently termed as non-renewable energy sources. But generation of hydro power requires water storage systems. As the conventional energy sources are present in limited amount generation of renewable energy sources like solar, tidal etc. is a great necessity of these days.

In this project we have modelled the standalone voltage source inverter first by using a DC source as input power and then instead of using direct DC source, a PV system is connected as input source and the output of the inverter is studied and analyzed. The unregulated DC output supply of the PV array is mainly because of changes in weather conditions. The maximum power is tracked with respect to irradiance levels and temperature by the help of DC-DC converter. The AC output voltage and frequency are regulated. Sinusoid pulse width modulation (SPWM) technique is implemented for voltage control for inverter and it is a closed loop control. For the design of inverter, its state space model is formulated and effects of various parameters like load resistance, controller gain and time constant is analyzed.

LIST OF FIGURES

Figure No.	Name of Figure	Page No.
1.1	Schematic diagram of standalone PV system	8
3.1	Basic constructional features of PV cell	11
3.2	Equivalent circuit of PV module	12
4.1	Typical I – V characteristics	14
4.2	Typical P – V characteristics	14
5.1	Boost converter circuit	17
5.2	Simulink PV module with converter	18
5.3	Output of PV array	19
5.4	Converter output	19
6.1	Inverter circuit diagram and signal of PWM modulator	21
6.2	Bode plot for different resistance value	26
6.3	Bode plot for different k_v	27
6.4	Bode plot for different t_v	27
6.5	Inverter Simulink block diagram	28
6.6	Reference signal	29
6.7	Carrier signal	29
6.8	Output voltage of inverter	29
6.9	Output current of inverter	30
6.10	Plot of state variables	30
6.11	FFT analysis of voltage waveform	31
6.12	FFT analysis of current waveform	31
7.1	PV system in Simulink	32
7.2	Converter output voltage when connected to inverter	32
7.3	Control voltage	32
7.4	Output voltage	33
7.5	Output current	33
8.1	Pin configuration of 33887 IC	35

LIST OF TABLES

Table No.	Name of Table	Page No.
6.1	Parameters used in simulation	25
6.2	Variation of GM, PM, GF, PF with load resistance	26
6.3	Variation of GM, PM, GF, PF with k_v	27
6.4	Variation of GM, PM, GF, PF with t_v	28
8.1	33887 Pin Definitions	35

1. INTRODUCTION

Renewable energy source are immense necessity in present as well as in future. Among various renewable energy systems, most important role is played by PV systems i.e. photovoltaic power generation systems as a clean power source to cope with the electricity demands in future. PV systems are widely used for generating power from solar energy. Of all renewable energy systems, PV based systems are the most eco-friendly energy solution for generating power. A schematic representation on PV system is shown in Fig.1.1.

The power delivered by the PV system is dependent on the radiance of solar energy and that vary time to time. So, the voltage and current and hence power delivered by the system is a variable quantity. To obtain maximum efficiency the maximum power point is tracked by applying an MPPT algorithm. The converter is used to obtain a constant output DC voltage which can be fed to an inverter to obtain alternating voltage which can be fed to a grid to meet the power demand of society.

But the output of a VSI is not a nice sinusoidal wave rather it is a square wave and we know from Fourier analysis square wave is the combination of sine waves of fundamental frequency its higher order harmonics. Before feeding to grid the harmonic components must be reduced which can be done by using SPWM for switching the MOSFETS or IGBTs used for switching and using inductive filter because high frequency switching techniques decreases lower order harmonics but increases higher order harmonics.

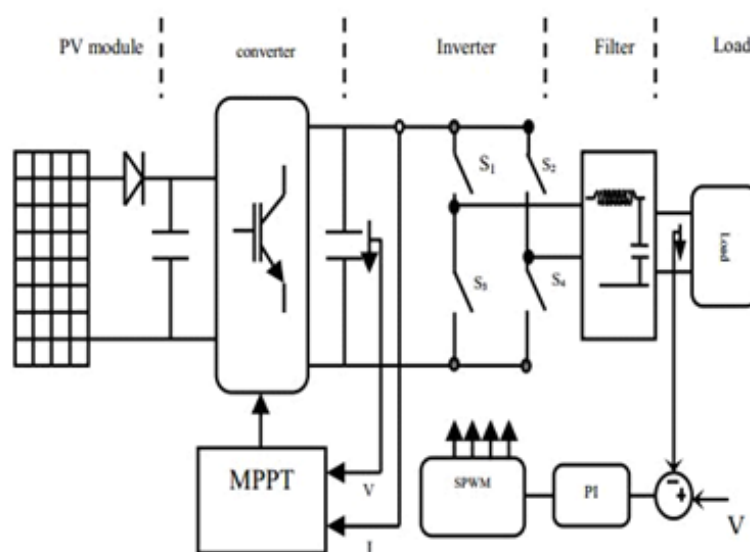


Fig. 1.1 Schematic diagram of standalone PV system

2. LITERATURE SURVEY:

Renewable sources of energy are also known as non-conventional type of energy. These sources can be replenished by naturally occurring processes. Examples of renewable energy sources are solar energy, geo thermal energy, bio-energy-bio-fuel, hydropower and wind energy etc. Sun and wind are bulk amount of renewable energy sources. In a PV system the light and heat energy that is available to us from sun is converted to electrical energy by the use of semiconductor material junctions.

World's leading economies have installed solar PV systems to produce power in range of MW. Solar PV systems can be availed in variety of sizes for various applications and are made up of semiconductor wafers. Solar cells combined to form solar arrays which can be regarded as the basic building block of PV system. As the efficiency of solar cells are very less power electronic components are used with it to harvest maximum efficiency. They can be installed on ground or on roof. Roof top installations offer good results if we are concerned about energy saving.

The tremendous potential associated with PV system is known over the years. Log Cabin Systems (LCS) and Urban Home Systems (UHS) are variety of technical arrangements (Dumais, 2010). In earlier days MI (micro-inverter) were basically multistage configured. A team of researchers in year 1996 presented an integrated power processing system with PV and it is called as an AC module. The power rating was 250 W. Following them, Kusakawa in 1998 introduced the concept of transformer less MI. Two staged inverter was designed by them and the inverter was directly connected to the PV module followed by a buck/boost converter. Low input voltage is provided by them to the switching devices; So MOSFETs are used with low conduction losses. The inverter Conduction losses are reduced and the efficiency is increased by the designing of a two stage MI which is based on Zero Voltage Switching inverter by M. Andersen and T.B. Alvesten in 1995. In 2008, a multilevel topology of inverter was proposed which does not inject DC to the grid. The methods of control using a two stage transformer less system are proposed by Franke et al. (2010) and they adopted a three phase H bridge inverter for interconnecting grids. A useful conclusion is drawn by his work i.e. the losses caused by current control PWM is less than the PI controller. But due to variance in switching frequency, the power quality reduces. A two stage micro inverter based on push pull converter with a single phase bridge inverter was designed by Trujillo et al. (2010, 2011). The bridge topology was not followed and switch numbers is reduced to two but they bear extra voltage which

results in requirement of higher rating. Thus control circuitry became simpler. Control scheme was prepared for a MI. In this scheme, MI worked as a current source and it operates as a voltage source for island mode.

Now-a-days the PV system is used in also hybrid energy systems with the tidal and wind energy systems. Because the load demand can be fulfilled at the time of need by all these systems if one system is not able to provide the required amount of load. The sun light is not available all the time and other energy sources are not available all the time, so these systems can be complementary to each other and if more amount of energy is available at a time we can save this in the form of chemical energy in batteries.

The solar cells can be modelled mathematically with the help of a current source with a parallel diode and a resistor in series and parallel to it. DC link capacitor is connected with it to maintain the voltage nearly constant and it can be connected with the boost converter which can be controlled by MPPT algorithm to track maximum power from the converter. The converter voltage is turned in to alternating by the use of an inverter.

3. PV SYSTEM

3.1 Solar energy

Solar energy is the most readily available form of energy. The radiant light from the sun and the heat is harnessed using technologies like photovoltaic, solar heating, thermal energy, artificial photosynthesis, etc. It is the most important of the non-conventional sources of energy and depending on the way they convert it into solar power, its technologies are characterized as either active or passive. Use of concentrated solar power, photovoltaic systems and solar water heating are included in active solar techniques whereas orienting a building to the sun is included in Passive techniques to harness the energy.

There are huge benefits in developing inexhaustible, affordable and clean solar energy technologies. Solar energy as an inexhaustible, indigenous and mostly import-independent resource has several advantages. These include enhanced sustainability, reduced pollution, lowered the costs of mitigating global warming and fossil fuels.

3.2 Photovoltaic cell

Generation of photovoltaic power involves the technology which converts thermal radiation from the sun directly into electricity through units called photovoltaic cells / solar cells. PV cells are usually made up of semiconductor materials with differently doped mono-crystalline as well as poly-crystalline silicon layer forming a pn junction. Thus a solar cell is nothing but a diode with a large surface area and a large area of pn junction. A basic cell configuration is shown in Fig.3.1.

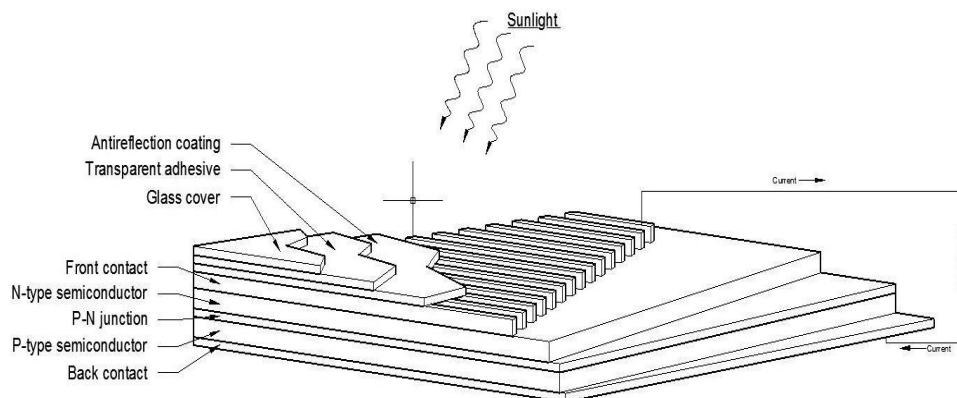


FIG.3.1 Basic constructional features of PV cell.

The load is connected to the cell through the metallic contacts. To enhance the absorption of radiation by reducing reflection, an antireflection coating of SiO_2 is applied on the top surface. For mechanical protection, the cell is placed under a glass cover and attached to it by a transparent adhesive. A single silicon solar cell with efficiency values between 15 – 18 % develops an open circuit voltage of the order of 0.65 V and generates a maximum current density between 35 – 40 mA / cm².

In a PV system, single solar cells are combined in series – parallel arrangement to form a PV Module, and several modules in series – parallel make a solar array.

3.3 Working principle

PV cell works on the principle of photoelectric effect which is defined as a phenomenon where sunlight of certain wavelength is absorbed by a matter leading to ejection of an electron from its conduction band. In PV cell, when light is absorbed by the pn junction, the energy of the absorbed photon is transferred to the electron system of the material. These results in the charge carrier generation which are separated at the junction. These carriers at the junction region are electron-hole pairs, which creates a potential gradient, gets accelerated under the effect of electric field and circulate as the current through an external circuit. The product of square of current with the circuit resistance gives the power which is converted into electricity. The rest power of the photons raises the cell temperature.

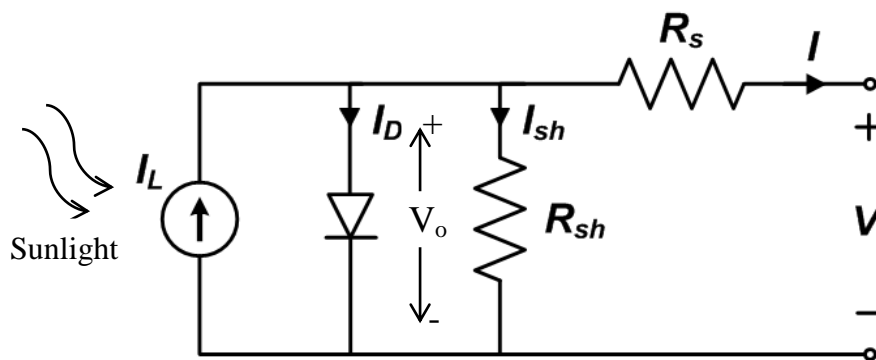


Fig. 3.2 Equivalent circuit of PV module

The equivalent circuit shown in Fig. 3.2 describes the physics behind PV cell. The circuit behaviour determines the output characteristics of PV cell. The effect of forward biasing of the pn junction is represented by the diode. The output current is given by

$$I = I_L - I_D - I_{sh}$$

$$= I_L - I_o \left[\exp\left(\frac{qV_o}{nKT}\right) - 1 \right] - \frac{V_o}{R_{sh}}$$

Where $V_o = V + IR_s$

V_o = voltage appearing across diode.

V = load voltage.

I_L = photo generated current.

R_s = internal (series) resistance of the system.

R_{sh} = shunt resistance

I_o = reverse saturation current of the diode.

T = Temperature in kelvin.

n = Ideality factor (≈ 1.92).

K = Boltzmann constant (1.38×10^{-23} J / K).

q = electronic charge (1.6×10^{-19} C).

When the is open circuited, i.e., when $I = 0$, the voltage V_o across the shunt branch appears as the open circuit voltage V_{oc} across the output terminals. Neglecting the effect of R_{sh} , the open circuit terminal voltage can be written as

$$V_{oc} = \frac{nKT}{q} \ln\left(\frac{I_L}{I_o} + 1\right)$$

4. MAXIMUM POWER POINT TRACKING

There is a poor overall efficiency when solar energy is converted into usable electrical energy using the PV system. Maximum power point tracking (MPPT) is a technique that is used to extract the maximum possible power from one or more photovoltaic modules and thus it increases the efficiency of the system. The relationship between solar irradiance, resistance and temperature produce a non-linear output. This relationship can be analyzed by the I-V curve. Due to the nature of the I-V characteristic, for a given solar insolation level and cell temperature, the output power is maximized at a specific load. The main purpose of the MPPT system is sampling the output of the PV cells for any given environmental condition. Proper resistance (load) is applied to obtain maximum power. MPPT devices are usually integrated into a converter system which provides voltage conversion or current conversion. They also help in regulation and filtering operation for various loads. The load may include power grids or batteries or motor drives. Fig 4.1 and Fig 4.2 shows the typical I-V characteristics and P-V characteristics of PV module respectively.

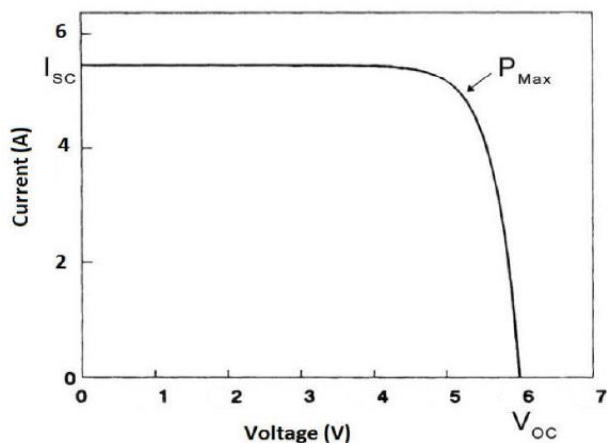


Fig. 4.1 Typical I-V characteristics

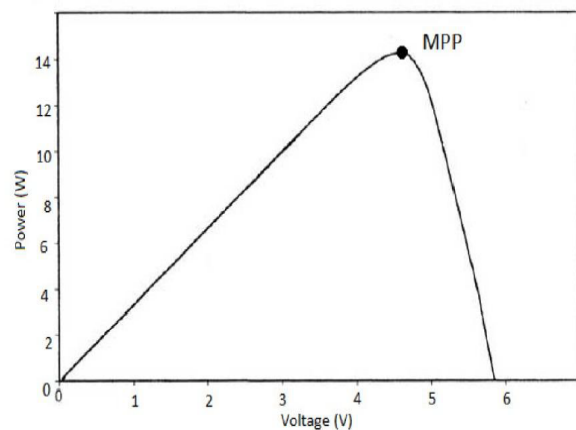


Fig. 4.2 Typical P-V characteristics

4.1. MPPT Techniques.

Maximum power point can be tracked using different techniques. Accuracy, simplicity, adaptability to temperature, adaptability to irradiance variation, relative implementation cost and control circuit complexity are some factors which determines their merits and limitations. Some techniques are explained as follows:

4.1.1 Control system with Voltage or Current reference.

In this method, a reference signal corresponding to maximum power point is used to compare the actual output voltage or current of the PV array. A PI controller is used for processing the error and its output is used for controlling the duty cycle of the PWM control signal which is further used for the dc-dc converter. In general, the maximum power point voltage is found to be 78% of the open circuit voltage. The corresponding current for maximum power point is around 90% of the short circuit current. The control loop can also use these values as reference.

4.1.2 Incremental conductance method.

This method shows that; at the maximum power point on the P-V curve, rate of change in power with respect to voltage is zero, i.e. $dP / dV = 0$. It can be also said that power is nearly constant with change in voltage. As $P = VI$ gives the output power, it can be concluded that

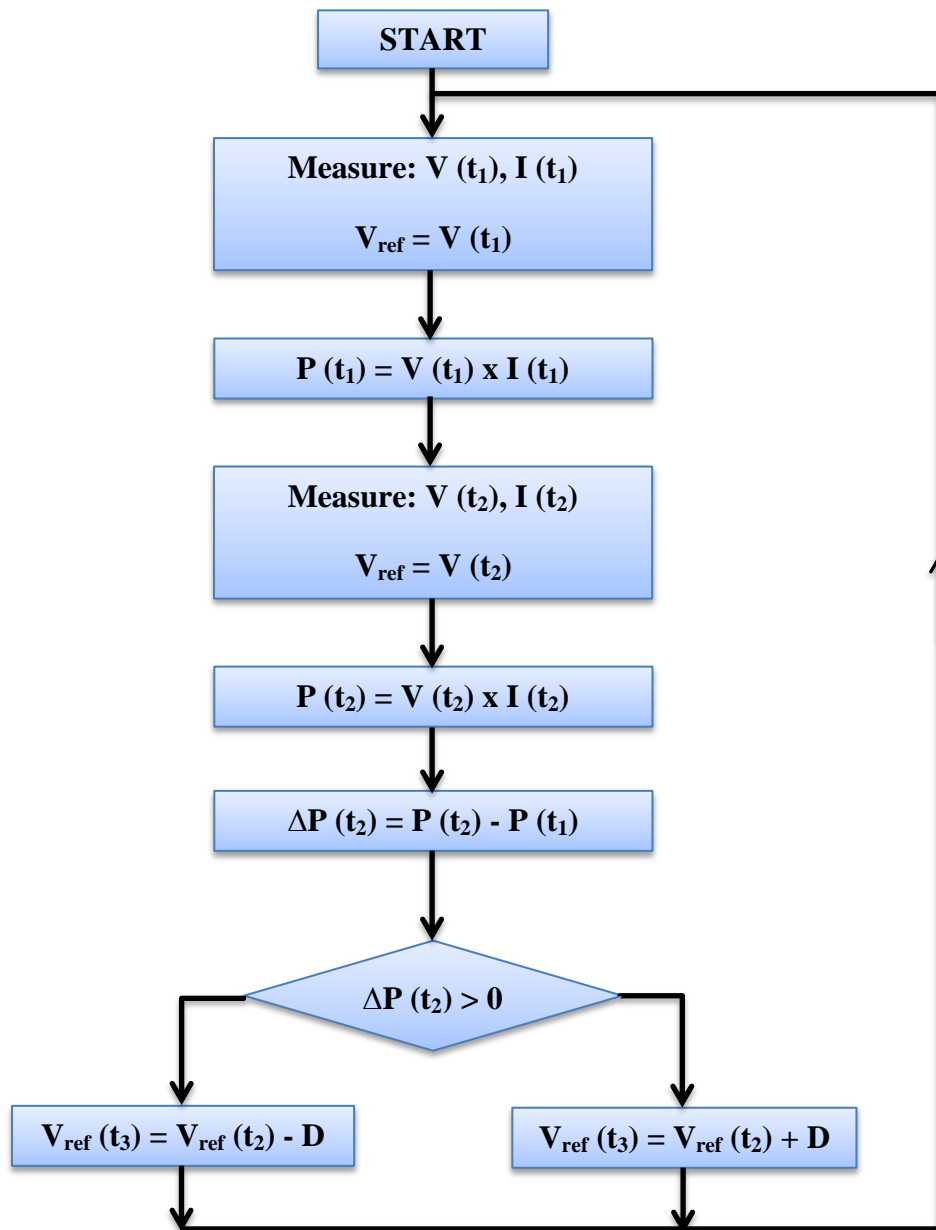
$$\frac{dI}{dV} = -\frac{I}{V}$$

The instantaneous conductance of the solar panel is represented in the left hand side. When instantaneous conductance becomes equal to the conductance of the solar cell then maximum power point is reached. There is elimination of the error occurring due to change in irradiance as both the current and voltage are sensed simultaneously. In this case, the complexity and the cost of implementation increases.

4.1.3. Perturb and Observe method.

The most commonly used MPPT technique is the Perturb and Observe method because of its ease of implementation. In this method, the voltage is increased as long as we get more power, i.e. the operating voltage is increased till dP / dV is positive. The operating voltage is decreased when dP / dV is negative. The voltage is kept constant if dP / dV is near to zero within a limit. This algorithm has a very less time complexity. It doesn't stop on reaching very close to the MPP, and keeps on perturbing.

4.2. MPPT Algorithm used - Perturb and Observe method.



5. DC – DC CONVERTER

Dc-Dc converters are used to control the step up and step down the DC voltage level. They are commonly known as choppers. The Boost converter increases the DC voltage level and Buck converter decreases the DC voltage level. It consists of one inductor, one switch and one diode basically. One capacitor should be connected across the load end to maintain the load voltage constant. The switching and duty ratio controls the DC output voltage of the converter. In buck converter the output is

$$V_o = KV_s$$

And in boost converter the output is

$$V_o = \frac{V_s}{1-K}$$

Where k is the duty cycle of the switching pulse. In PV module the output of the solar cell is not directly fed to the Inverter. It is first stepped up to a suitable voltage and then fed to the Inverter module.

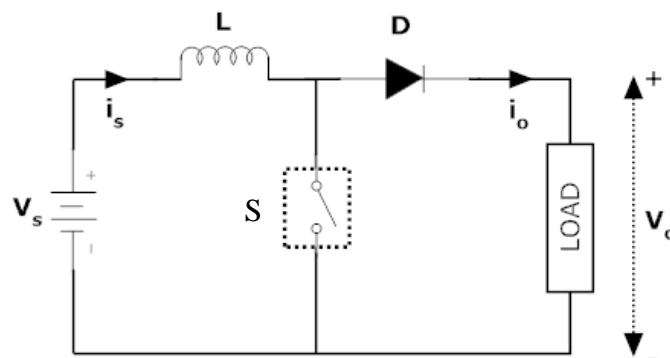


Fig.5.1. Boost converter circuit

5.1. Working principle:

Fig.5.1. illustrates an elementary form of a boost converter. When the switch S is on, a closed path of current is formed and the inductor stores energy during the period T_{on} . When it is off, the inductor current cannot die instantaneously, and thus flows through the diode and the load for the period T_{off} . The polarity of the induced emf in inductor is reversed as the current decreases. As a result load voltage V_o exceeds the source voltage V_s . In this manner the step up converter operates and the stored energy in inductor is released to the load.

During T_{on} , $V_L = V_S$ and $V_o = 0$; where V_L = voltage across inductor and V_o = load voltage.

During T_{off} , $V_o = V_L + V_S$

The average output voltage across the load is given by

$$V_o = \frac{V_S}{1-K} \quad , \text{ where the duty cycle } K = \frac{T_{on}}{T_{on}+T_{off}}$$

5.2. Simulink model and Results.

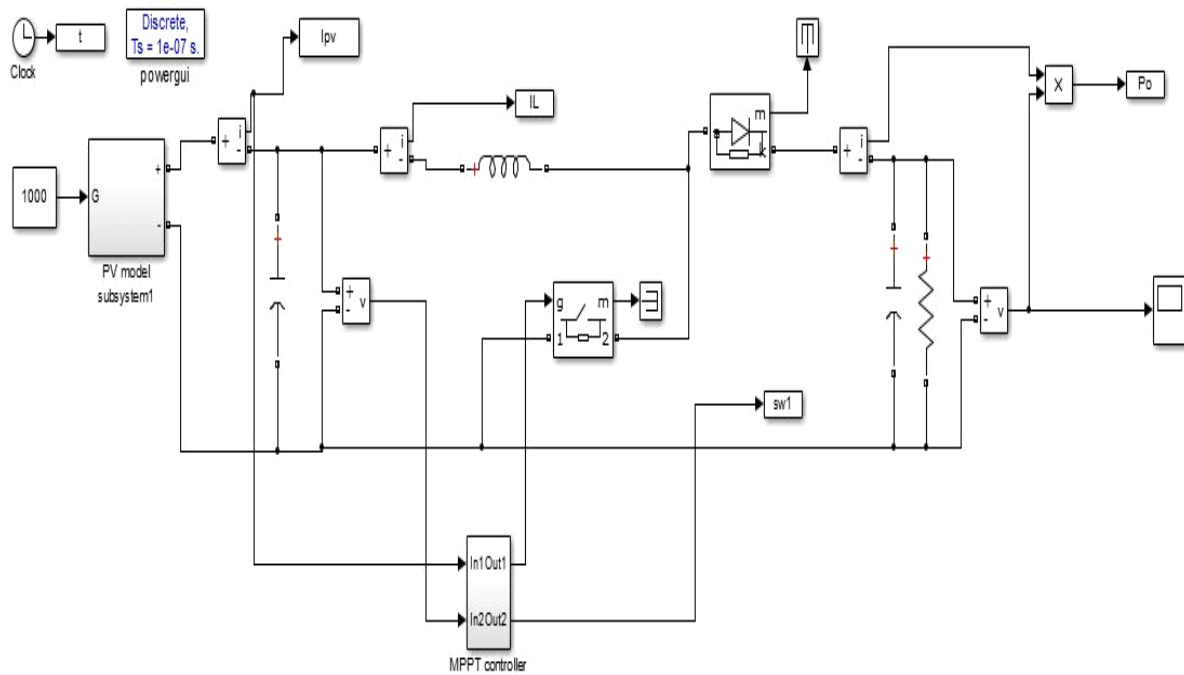


Fig. 5.2. Simulink PV module with converter

Parameters:

$C1 = 0.1 \mu\text{F}$; $L = 140 \text{ mH}$; $C2 = 1000 \mu\text{F}$; $R = 20 \Omega$

Output:

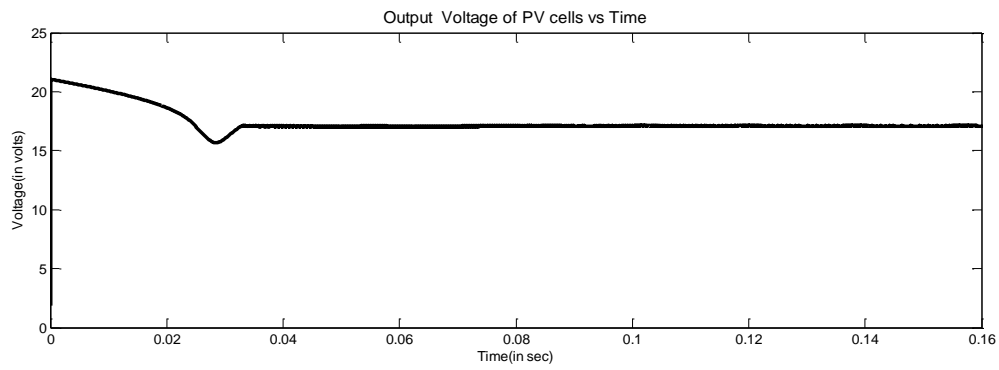


Fig 5.3 output of PV array

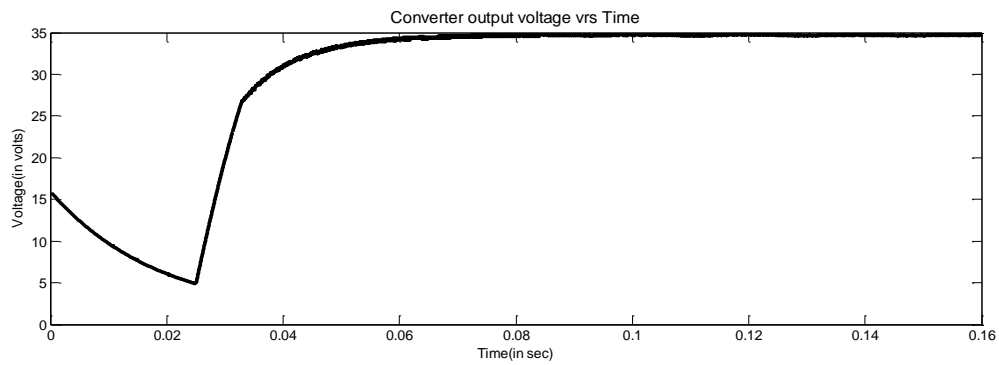


Fig. 5.4 converter output.

In the fig.5.3 the output of PV array with respect to time is shown when the solar irradiance is 1000 W / m^2 . The output voltage obtained is nearly 17 V. This voltage is stepped up to 35 V using the boost converter. The converter output with respect to time is shown in fig.5.4.

6. INVERTER

A full bridge inverter as shown in Fig.6.1 Consists of four switches (MOSFET). When switch S1, S4 conduct, load voltage becomes equal to source voltage. When switch S2, S3 conduct voltage across load is negative of source voltage. When the inverter operates it should always be ensured that the two MOSFETs in the same branch do not conduct simultaneously because this would result to a direct short circuit of the source which will cause high current through source. For resistive load, load current and load voltage are always in phase with each other. For inductive loads, load current will not be in phase with the load voltage and the diodes which are connected in antiparallel with MOSFETs will allow the flow of current to at the instance when the main MOSFETs are turned off. These diodes are called feedback diodes. So in case of resistive loads the current waveform will follow voltage wave form but if purely inductive loads are used the waveform will be triangular in nature.

In sinusoidal pulse modulation (SPWM), in each half cycle several pulses are used. The pulse width is determined by a sinusoidal function of the angular position of the pulse in a cycle. For the realization of SPWM, sinusoidal reference wave is compared with a high frequency triangular carrier wave. Both the waves are fed to a comparator. The comparator output is high, only when the sinusoidal wave has magnitude higher than the triangular wave, otherwise it is low. The trigger pulse generator processes the output of comparator in such a way that the output voltages of the inverter have a pulse width in accordance to the output pulse width of the comparator.

Modulation index (MI) in this case is defined by the ratio of V_r / V_c and the harmonic content of the output wave is controlled by it. Here V_r and V_c represents the magnitude of reference and carrier signal respectively. The control of output voltage is done by varying the MI.

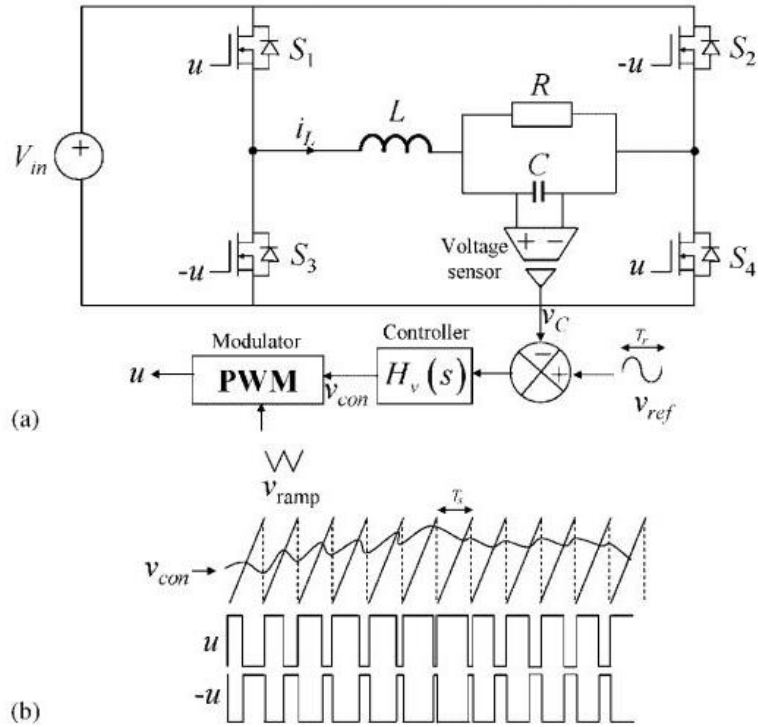


Fig. 6.1 Inverter. (a) Circuit diagram. (b) Representative signal of the PWM modulator.

The above Fig.6.1 shows the schematic diagram of a DC-AC inverter. The switches are activated as follows, switch S1 and S4 are driven simultaneously while switch S2 and S3 are switched on in alternate fashion to switch S1 and S4. To sense the output voltage, a voltmeter or a voltage sensor is there and the error in voltage is represented by the voltage difference $V_{ref} - V_o$. This error is processed using a voltage controller which is in form of a low-pass filter or dominant pole. V_{con} is the output of the controller, which is then connected to the non-inverting input of the comparator. Here the inverting input is applied to saw tooth ramp generator, in such a way that in steady state the switches S1 and S4 are activated at each switching cycle while they are turned OFF when the ramp voltage $V_{ramp}(t)$ crosses the control signal $V_{con}(t)$. Waveforms of state variables are periodic and are obtained by analyzing the circuit. Here the steady state dynamics is characterized by two periods namely: the reference voltage period T_r and the switching period T_s . Therefore the stationary periodic attractor is settled into a two dimensional torus which is characterized by two periods, which are the line reference period and the switching period.

During first phase when S1 and S4 are closed, the state equations for voltage and current are given by

$$\frac{dV_C}{dt} = -\frac{1}{RC}V_C + \frac{1}{C}I_C$$

$$\frac{dI_L}{dt} = \frac{1}{L}(V_{in} - V_C)$$

During second phase when S1 and S4 are open, the state equations are as follows:

$$\frac{dV_C}{dt} = -\frac{1}{RC}V_C + \frac{1}{C}I_C$$

$$\frac{dI_L}{dt} = -\frac{1}{L}(V_{in} + V_C)$$

Where L denotes the inductance, R is load resistance, C is capacitance of the capacitor, I_L denotes the inductor current, V_C is the output capacitor voltage and V_{in} is the input voltage.

6.1. Modelling of output voltage controller:

To track the output voltage V_C , a desired sinusoidal reference voltage $V_{ref} = V_r \sin(Wr t)$ is used. We have used an outer voltage loop controller which is in the form of a dominant pole (low pass-filter). As it is a low pass filter higher order frequencies and noise can be filtered by it. To obtain less ripple in the feedback control voltage the design parameter crossover frequency $f_v=1/t_v$ is adjusted suitably together with other parameters. In frequency domain, the small signal transfer function for this controller can be represented as:

$$H_v(s) = \frac{V_{con}(s)}{V_{error}(s)} = \frac{k_v}{1 + s t_v}$$

Here $V_{error} = V_{ref} - V_C$

k_v is the DC gain of the filter which is also known as velocity error constant. Another state variable for the system defined by this dynamic controller whose dynamic behaviour is given by:

$$\frac{dV_{con}}{dt} = \frac{1}{t_v}(-V_{con} + k_v(V_{ref} - V_C))$$

6.2. Compact expression for the exact switched model:

The system model which is switched can be written as:

$$\dot{X} = AX + B1(t) \quad \text{During phase 1}$$

$$\dot{X} = AX + B2(t) \quad \text{During phase 2}$$

The system matrices and system vectors are given as:

$$A = \begin{bmatrix} -\frac{1}{RC} & \frac{1}{C} & 0 \\ -\frac{1}{L} & 0 & 0 \\ -\frac{kv}{t_v} & 0 & -\frac{1}{t_v} \end{bmatrix}; B1(t) = \begin{bmatrix} 0 \\ \frac{V_{in}}{L} \\ \frac{kv}{t_v} V_r \sin(w_r t) \end{bmatrix}; B2(t) = \begin{bmatrix} 0 \\ -\frac{V_{in}}{L} \\ \frac{kv}{t_v} V_r \sin(w_r t) \end{bmatrix}$$

The switching decision is taken into account and it is considered that control signal can take values from the set [0, 1]. Now the system switched model of the system can be expressed as

$$\frac{dX}{dt} = AX + (B1(t) - B2(t)) \left[\frac{1}{2} + \frac{\text{sign}(V_{con} - V_{ramp}(t))}{2} \right] + B2(t)$$

Which is actually a nonlinear model and hard to solve by conventional methods.

6.3. Transferring the model into small signal averaged model:

A discontinuous switched vector field is represented by the above equation. The discontinuous signal $u(t)$ which drives the system makes it the system nonlinear. To solve this type of nonlinear equations basically two different types of methods are there. One traditional approach is to study its dynamical behaviour by solving the discontinuous equation numerically and then simulating the system behaviour for different parametric values under various operating points.

But this method is disadvantageous being computationally intensive. It will take a lot of time to solve it and it will consume more memory. Second approach is to take the average of the system equation over a switching period which will remove the discontinuity which is caused due to the switching action.

This can be simplified further. The reference signal can be considered to be constant and its RMS value is used to replace it. This way, the slow-scale dynamical behaviour can be concluded and can be drawn obtaining the small signal transfer function.

For our system the switched signal $u(t)$ is replaced by its average over the duty cycle, and hence the averaged model which is continuous is obtained and is given by

$$\frac{dX}{dt} = AX + (B1(t) - B2(t)) \frac{1}{2} \left(\frac{V_{con}(t)}{V_u - V_l} + 1 \right) + B2(t)$$

Where $V_u = 1v$ and $V_l = -1v$

Now the new linear time varying model is:

$$\frac{d}{dt} \begin{bmatrix} \overline{V_C} \\ \overline{I_L} \\ V_{con} \end{bmatrix} = \begin{bmatrix} -\frac{1}{RC} & \frac{1}{C} & 0 \\ -\frac{1}{L} & 0 & \frac{1}{L} \left(\frac{V_{in}}{V_u - V_l} \right) \\ -\frac{kv}{t_v} & 0 & -\frac{1}{t_v} \end{bmatrix} \begin{bmatrix} \overline{V_C} \\ \overline{I_L} \\ V_{con} \end{bmatrix} + \begin{bmatrix} 0 \\ 0 \\ \frac{kv}{t_v} V_{ref} \end{bmatrix}$$

This model is solved in MATLAB and the output is observed. To see the effects due to the change of different parameters i.e. load resistance, gain kv and t_v the small signal transfer function is obtained and i.e. given by:

$$G(s) = \frac{c(s)}{V_{ref}(s)} = \frac{kvV_{in}W_0^2}{(V_u - V_l)(1 + st_v)(s^2 + 2\zeta W_0^2 s + W_0^2)}$$

Here $W_0 = \frac{1}{\sqrt{LC}}$ and $\zeta = \frac{1}{2R} \sqrt{\frac{L}{C}}$

The gain margin and phase margin of the system can be obtained from the bode plot for different values of load resistance, gain kv and time constant t_v . We can take 12, 24, 36, 48, 110, 125 and 250 V as nominal input values for DC to AC inverters. We have used voltage $V_{in} = 36$ in this project an input.

To design DC to AC there are other important output specifications to be considered which are maximum voltage, maximum power, maximum steady-state current and frequency range. In the function of the application, the peak-to-peak output reference voltage or its equivalent RMS value is set. The load R determines the maximum power consumed by load and also the steady-state load current.

To choose the inductor value L of the filter, the voltage drop across the inductor is considered to be less than 1% of the output voltage of the inverter, i.e.

$$W_r L < 0.01 R$$

The output capacitor will decide the frequency range, which is chosen for system to have a resonance frequency denoted by W_o :

$$C = \frac{1}{W_o^2 L}$$

Finally, the selection of switching frequency is done such a way that $10W_o < W_s = 2\pi f_s$. By taking into account these considerations, the value of the circuit parameters are taken on account of these considerations. All the required parameters are shown in Table 6.1. A desired phase margin is obtained by selecting a proper value of k_v .

TABLE 6.1: Parameters used in simulation

PARAMETER	VALUE
V_{in}	36 V
L	200 μ H
C	10 μ F
R	[5 ,20] Ω
F_r	50 Hz
F_s	50 KHz
V_l	-1 V
V_u	1 V
V_r	28 V
K_v	[0.4, 1.4]
T_v	[10 μ sec,10 ms]

Then the actual nonlinear model is simulated in MATLAB Simulink by taking appropriate values of all parameters and the results i.e. the output voltage and current waveforms are obtained and observed. Now the output of the converter is given as input to the inverter and the output voltage and current along with the output of PV model waveform behaviour is studied.

6.4. Effect of variation of different parameters upon inverter.

By considering all the parameters, different plots are performed to show the important aspects concerning the stability of the system as well as its performance.

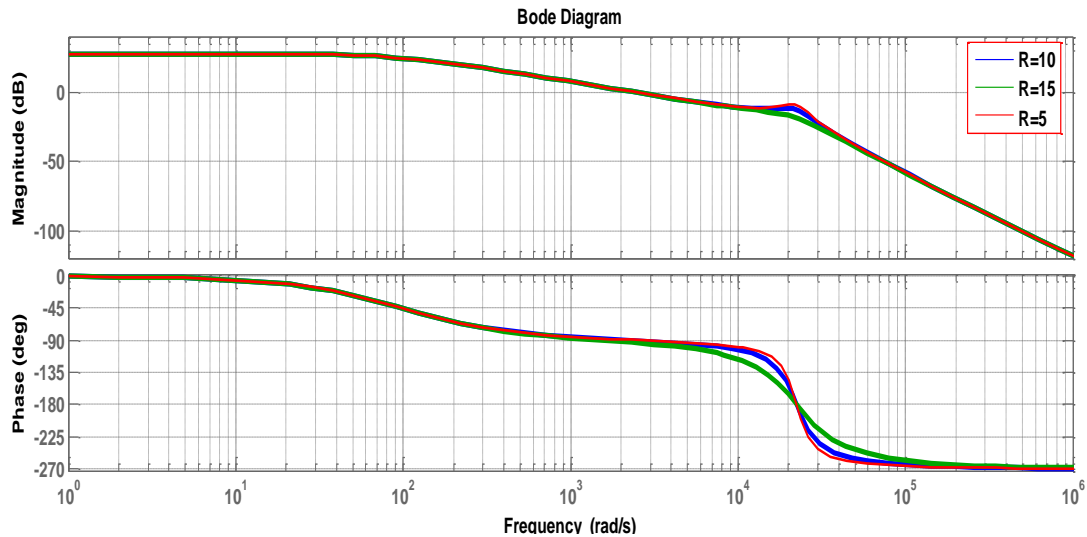


Fig.6.2. Bode plot for different resistance value

TABLE 6.2: Variation of GM, PM, GF, PF with load resistance

R (in Ω)	Gain margin (dB)	Phase margin (in deg.)	Gain cross over frequency (rad/s)	Phase cross over frequency (rad/s)
5	8.5814	86.9945	2.3537×10^3	2.2405×10^4
10	4.2822	89.6897	2.3617×10^3	2.2383×10^4
15	2.8529	90.5977	2.3633×10^3	2.2376×10^4

From Fig.6.2 it is observed that with increase in resistance the gain cross-over frequency and phase crossover frequency does not change a lot but phase margin increases and gain margin decreases.

But the increase in phase margin is not much with respect to decrease in gain margin. So the system drives towards instability with increase in resistance. So the resistance value chosen for the inverter as load is 5 ohms.

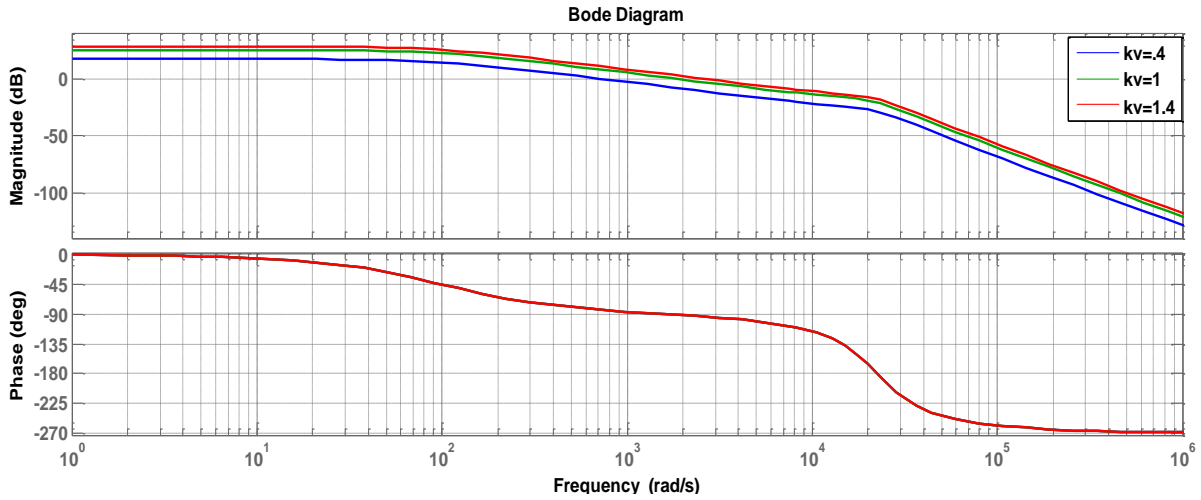


Fig. 6.3. Bode plot for different K_v

TABLE 6.3: Variation of GM, PM, GF, PF with K_v .

K_v	Gain margin (dB)	Phase margin (in deg.)	Gain cross over frequency (rad/s)	Phase cross over frequency (rad/s)
0.4	27.8895	96.3429	0.7134×10^3	2.2405×10^4
1	11.1558	89.0172	1.8043×10^3	2.2405×10^4
1.4	7.9684	86.3847	2.5379×10^3	2.2405×10^4

Fig.6.3. shows that the phase response and hence the phase crossover frequency doesn't change but gain crossover frequency increases. The gain margin decreases sharply with increase in K_v . The phase margin also decreases but to minimize the value of steady state error, K_v should be somewhat greater. So the value of k_v chosen for the simulation is 1.3.

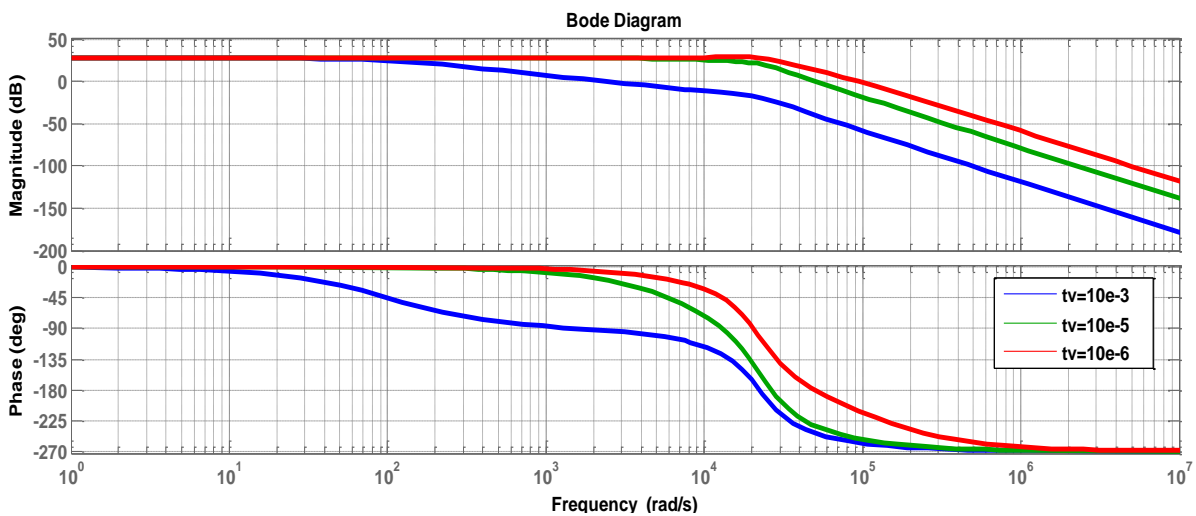


Fig.6.4. Bode diagram for different t_v

TABLE 6.4: Variation of GM, PM, GF, PF with t_v .

t_v (time constant in s)	Gain margin (dB)	Phase margin (in deg.)	Gain cross over frequency (rad/s)	Phase cross over frequency (rad /s)
10×10^{-3}	8.584	86.9945	2.3537×10^4	2.2405×10^3
10×10^{-5}	0.2137	-30.4794	5.0410×10^4	2.6458×10^4
10×10^{-6}	0.1368	-52.4936	9.3911×10^4	5.0000×10^4

In fig.6.4.bode plot for different values of time constant (t_v) of controller transfer function is plotted. Here the gain and phase cross over frequencies increases with decrease in time constant. The gain margin decreases with t_v varying from 10 ms to 10 μ s. Phase margin is positive for $t_v = 10$ ms and becomes negative for $t_v = 100 \mu$ s and decreases further if the time constant is decreased. So it is better to have t_v near to 10 ms. Near 10 μ s gain margin is very close to zero and phase margin is also negative, hence system is more prone towards instabilities.

6.5. Inverter model and results:

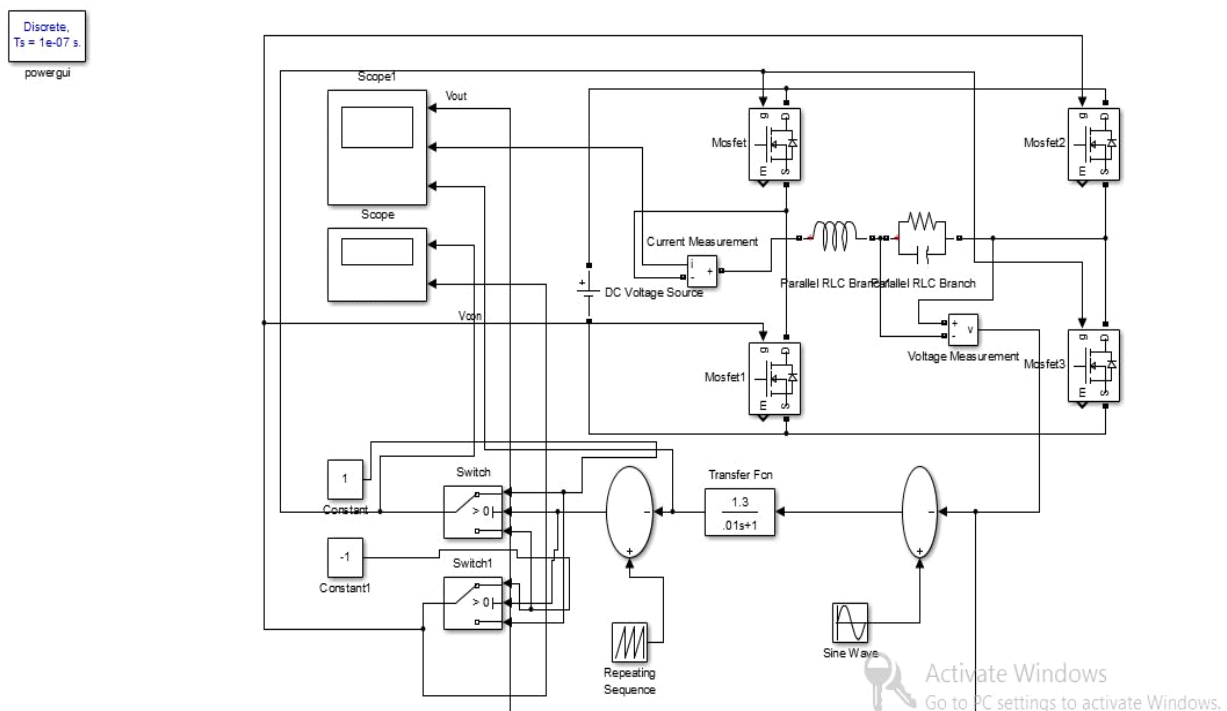


Fig.6.5 The inverter Simulink block diagram

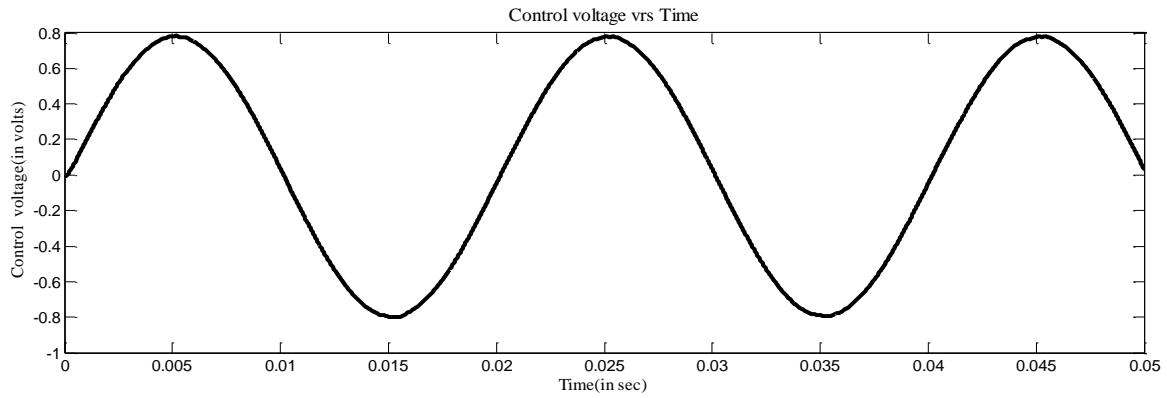


Fig.6.6. reference signal

The above signal shown in fig.6.6 is generated using the error signal i.e. $V_{ref} - V_{out}$ and the controller. This acts as the reference for the generation of switching pulses.

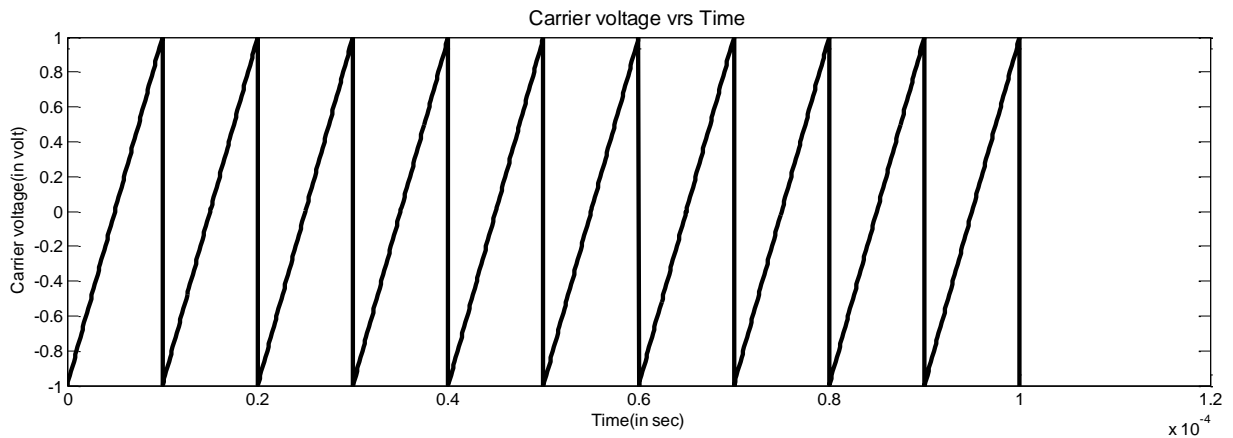


Fig. 6.7. Carrier signal

The above signal acts as a carrier for the generation of switching pulses. Its frequency is 50 KHz and peak to peak amplitude is 2 V.

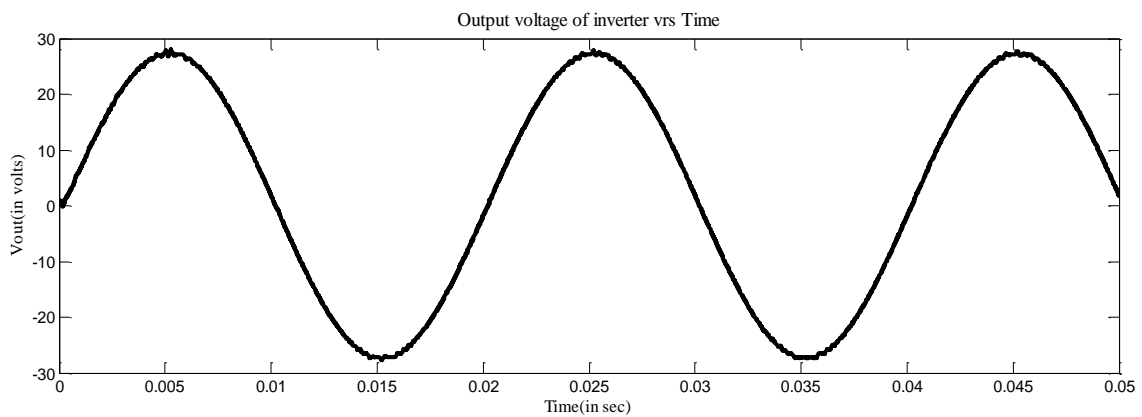


Fig. 6.8. Output voltage of inverter.

This output in fig. 6.8 is obtained when the input is a dc of voltage 35 V.

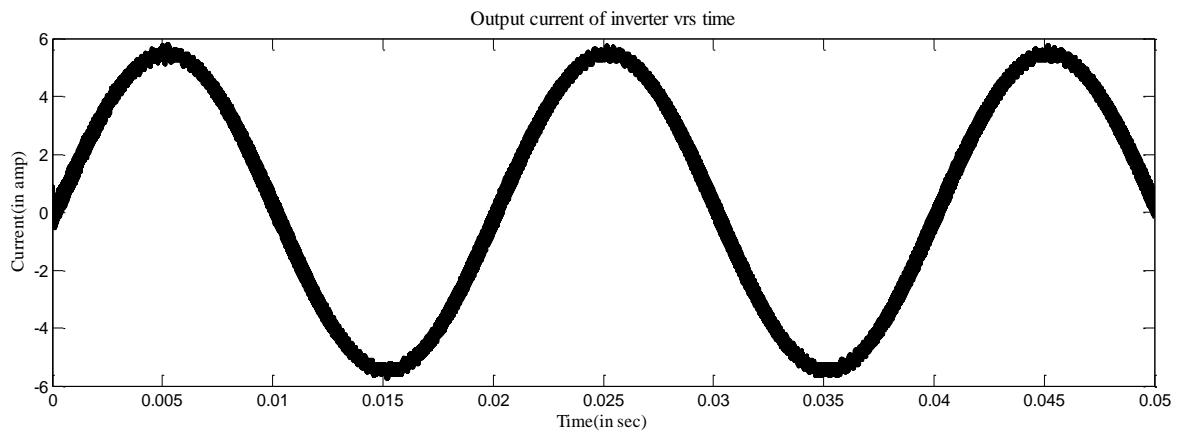


Fig. 6.9 Output current of inverter.

The output current of the inverter with respect to time is plotted above.

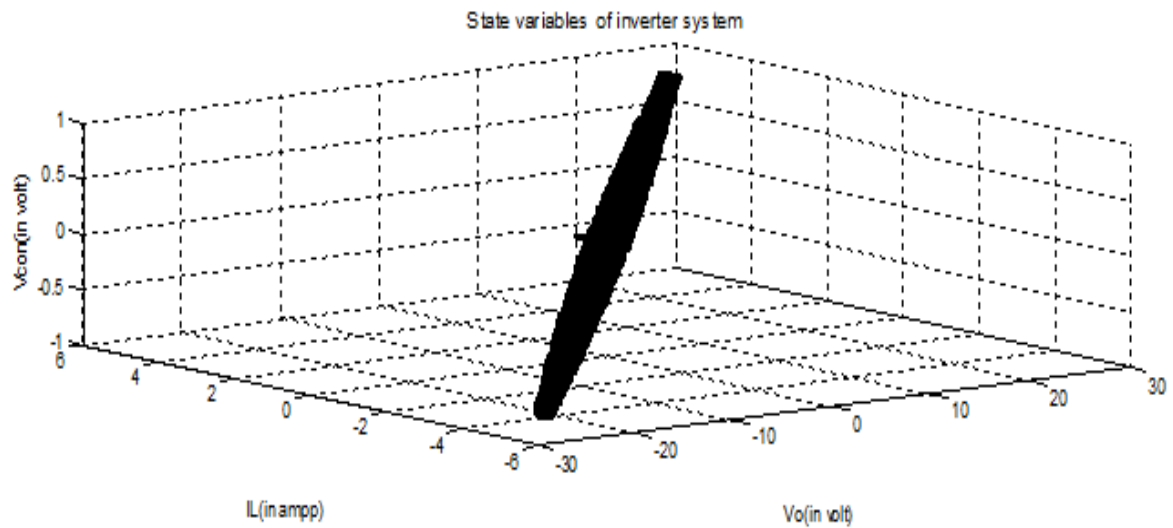


Fig. 6.10. Plot of state variables

In the above figure, the three state variables namely voltage across load, inductor current and the control signal voltage is plotted.

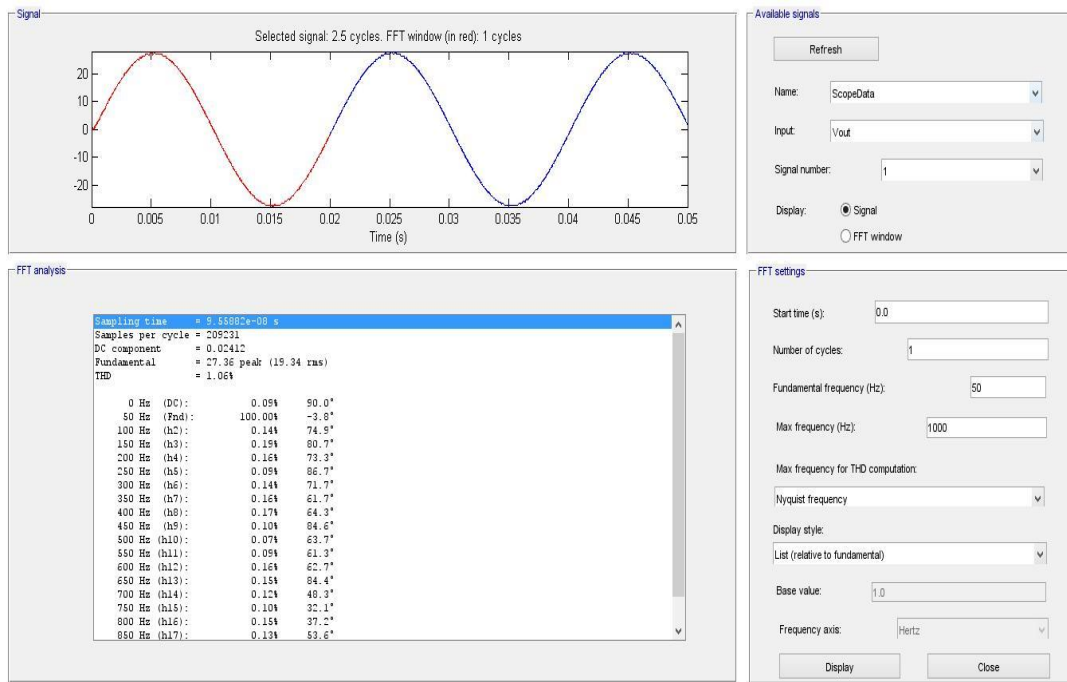


Fig. 6.11 FFT analysis of voltage waveform

The Fourier transform of the voltage waveform is obtained to know the harmonic frequency contents in the voltage waveform. The total harmonic distortion in this case is found to be 1.06%.

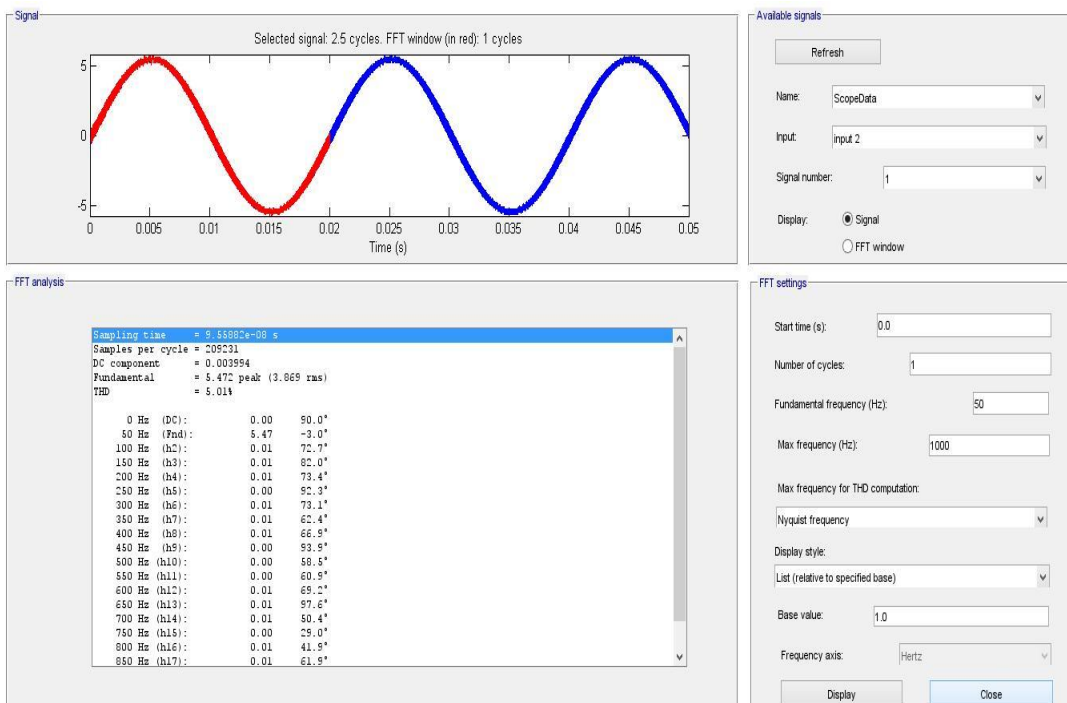


Fig. 6.12 FFT analysis of current waveform

From the FFT analysis of the current waveforms shown in fig.6.12, it is found that harmonic content i.e. THD in this case is 5.01%.

7. SIMULINK MODEL OF PV SYSTEM

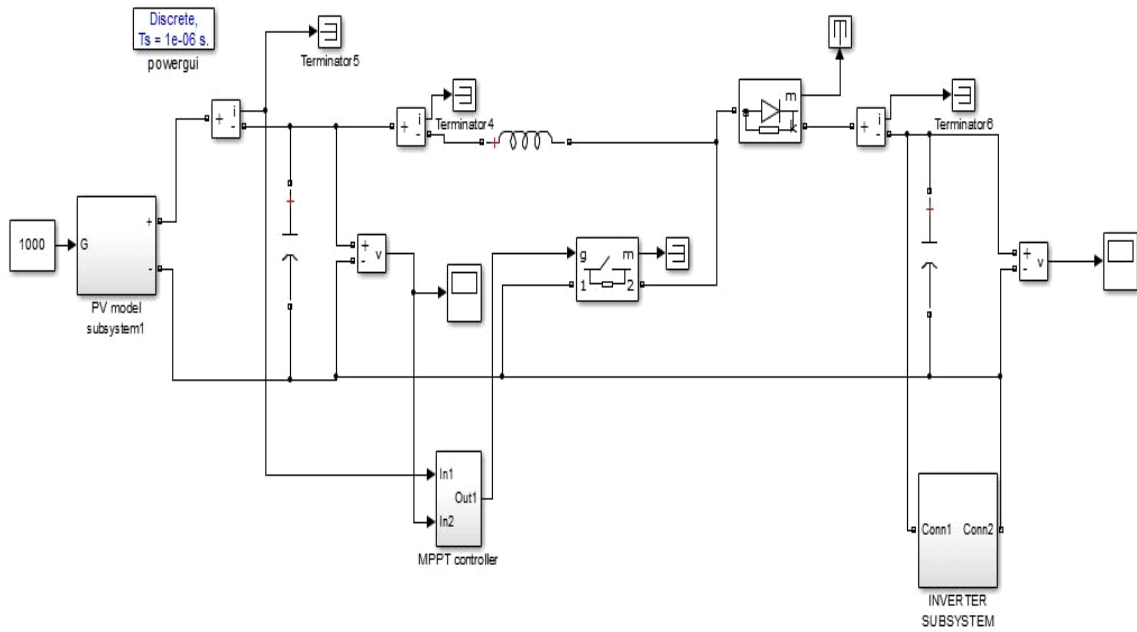


Fig.7.1 PV system in Simulink

7.1 Results

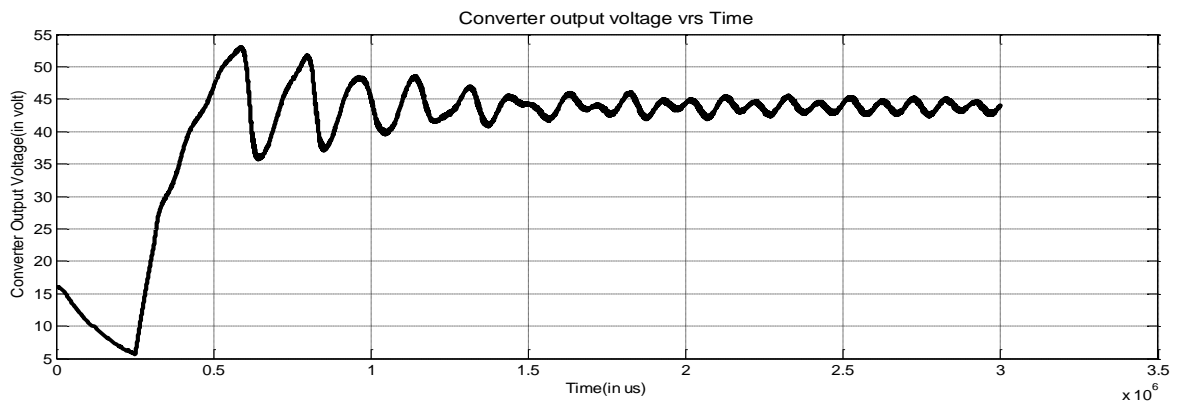


Fig. 7.2 converter output voltage when connected to inverter.

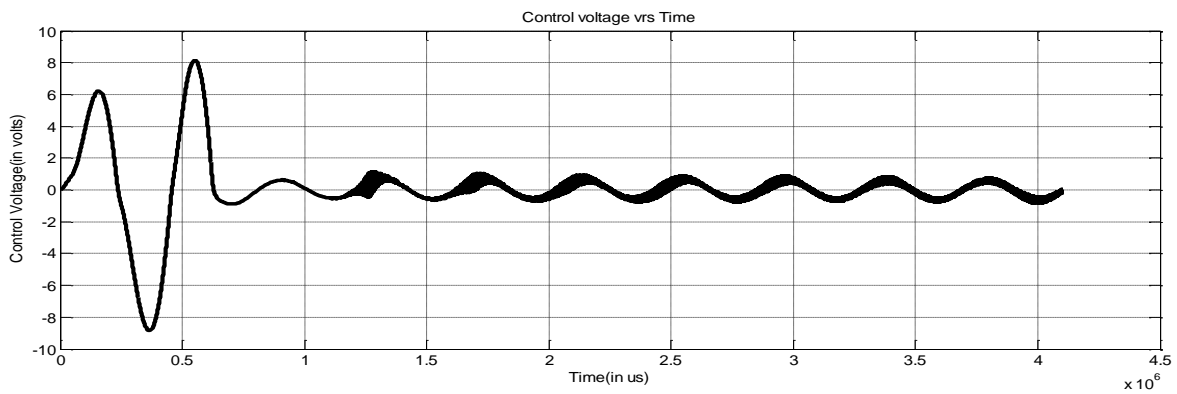


Fig. 7.3 control voltage

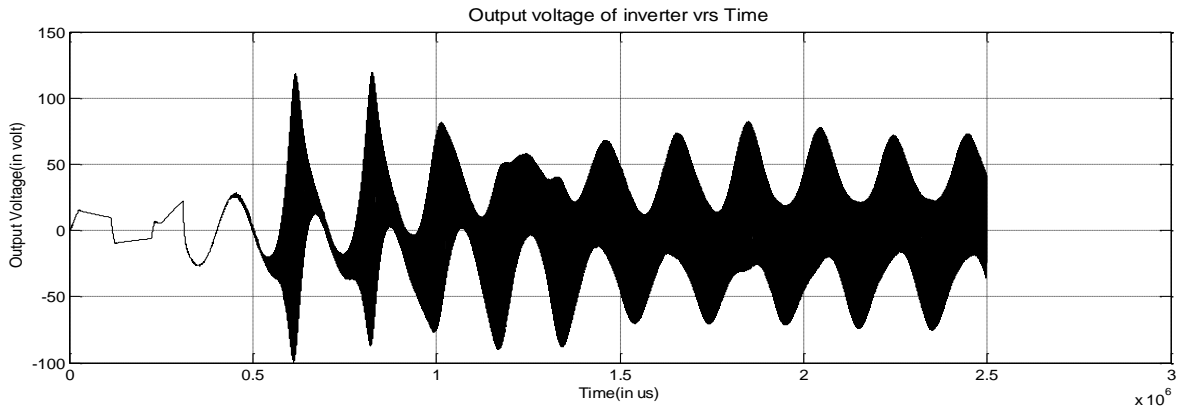


Fig. 7.4 output voltage

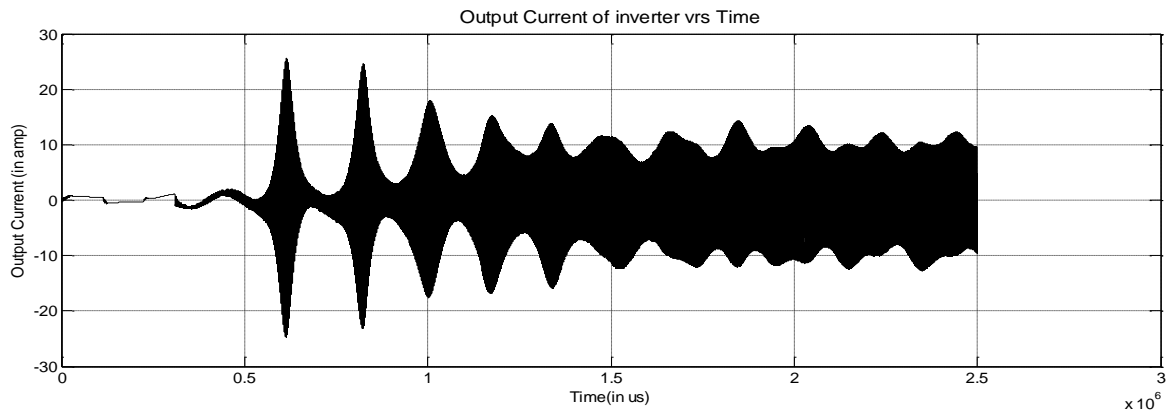


Fig. 7.5 Output current

The above figures show the output voltage of converter connected to PV array, the control voltage used as the reference for the switching, the output voltage and current of the inverter. It is found that even after a long interval of time there is very much instabilities in the system for which the output does not comes to a constant value.

Since the PV output is not constant and distorted, corresponding output waveform (current, voltage as well as controller voltage) of the inverter circuit is also not sinusoidal and full of distortion which can be easily observed in fig.7.4 and fig.7.5.

8. H – BRIDGE INVERTER IC (33887)

The 33887 is a monolithic H-Bridge Power IC with a load current feedback feature making it ideal for closed-loop DC motor control. The IC incorporates internal control logic, gate drive, charge pump, and low $R_{DS(ON)}$ MOSFET output circuitry. Output loads can be pulse width modulated (PWM-ed) at frequencies up to 10 kHz. The load current feedback gives a proportional (1/375th of the load current) constant-current output suitable for monitoring using a microcontroller's Analog / digital input. This IC is able to control inductive loads with continuous DC load currents up to 5.0 A. Also the peak active current is between 5.2 A and 7.8 A. The design of closed-loop torque/speed control as well as open load detection is facilitated by this feature.

An output Fault Status pin reports short circuit, under-voltage, and over-temperature conditions. The polarity control of two half-bridge totem-pole outputs is provided by two independent inputs. Two disable inputs force the H-Bridge outputs to tri-state where it exhibit high impedance. The parameters of this IC is specified over a temperature range of -40°C to 125°C and a voltage range of 5 V to 28 V.

8.1. Features

- Operation voltage between 5 V to 28 V
- Operation with poor performance up to 40 V
- H-Bridge MOSFETs with $R_{DS(ON)}$ of 120 m Ω
- Compatible Inputs : TTL/CMOS
- Active Current Limiting Regulation
- PWM Frequencies up to 10 kHz
- Sleep Mode with Current Draw $\leq 50 \mu\text{A}$
- Fault Status Reporting

8.2. Pin configuration.

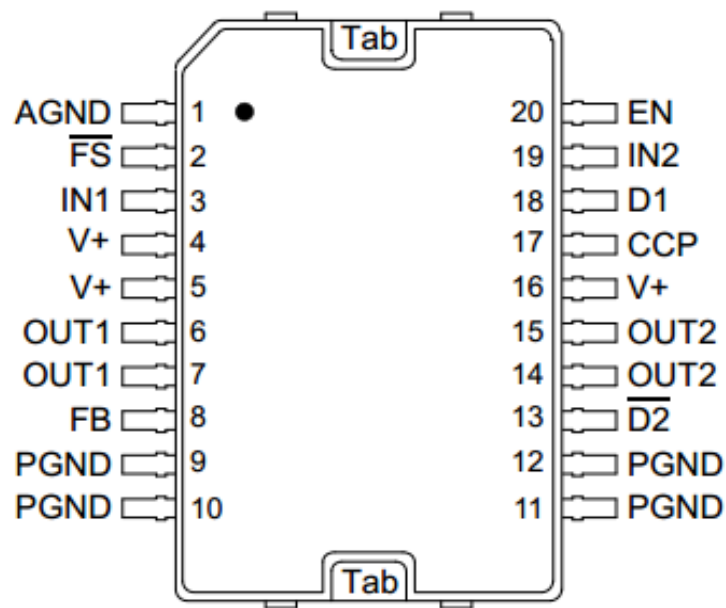


Fig.8.1. pin configuration of 33887 IC

Table 8.1 33887 pin definitions

Pin	Pin Name	Formal Name	Definition
1	AGND	Analog ground	Low-current analog signal ground
2	FS	Fault Status for H-Bridge	Open drain active LOW Fault Status output requiring a pull-up resistor to 5.0 V.
3	IN1	Logic Input Control 1	Logic input control of OUT1 (i.e., IN1 logic HIGH = OUT1 HIGH).
4,5,16	V+	Positive Power Supply	Positive supply connections
6,7	OUT1	H-Bridge Output 1	Output 1 of H-Bridge.
8	FB	Feedback for H-Bridge	Current sensing feedback output providing ground referenced 1/375 th of H-Bridge high-side current.
9 – 12	PGND	Power Ground	High-current power ground.
13	D2	Disable 2	Active LOW inputs used to simultaneously tri-state disable both H-Bridge outputs. When D2 is Logic LOW, both outputs are tri-stated.
14,15	OUT2	H-Bridge Output 2	Output 2 of H-Bridge.
17	CCP	Charge Pump Capacitor	External reservoir capacitor connection for internal charge pump capacitor.

Pin	Pin Name	Formal Name	Definition
18	D1	Disable 1	Active HIGH input used to simultaneously tri-state disable both H-Bridge outputs. When D1 is Logic HIGH, both outputs are tri-stated.
19	IN2	Logic Input Control 2	Logic input control of OUT2 (i.e., IN2 logic HIGH = OUT2 HIGH).
20	EN	Enable	Logic input Enable control of device (i.e., EN logic HIGH = full operation, EN logic LOW = Sleep Mode).
Tab / pad	Thermal Interface	Exposed Pad Thermal Interface	Exposed pad thermal interface for sinking heat from the device. Note Must be DC-coupled to analog ground and power ground via very low impedance path to prevent injection of spurious signals into IC substrate.

9. CONCLUSION:

Micro-inverter technology is an upcoming field having lot of scope for research. Here we have designed a standalone micro inverter circuit and simulated it using Simulink. The parameters of the inverter model like the inductance, the dc gain (k_v) and time constant (t_v) considerably affect the system dynamics at the switching time and should be chosen properly to obtain a stable periodic behaviour.

When instead of PV, DC source is connected the voltage waveform is quite similar to the reference voltage but both current and voltage has some harmonic content in them. After connecting the PV module the harmonic content in current and voltage increased and the output of the PV was also affected considerably.

10. REFERENCES

- [1]. Abdelali El Aroudi, Enric Rodriguez, Mohamed Orabi and Eduard Alarcon, “Modelling of switching frequency instabilities in Buck – Based DC – AC H – Bridge Inverters”, International Journal of Circuit theory and applications, 2011, no. 39, pp. 175 – 193.
- [2]. Abdelali El Aroudi, Eduard Alarcon, Enric Rodriguez and Mohamed Orabi, “Modeling of Switching Frequency Instabilities in Buck-Based DC-AC Inverters by Nonlinear Time Varying Poincare Mappings”, power system conference, March 2008. MEPCON 2008, 12th International middle east, pp. 354 – 359.
- [3]. S. Senthil Kumar, Ganesh Dharmireddy, P.Raja, S.Moorthi, “A Voltage Controller in Photo-Voltaic System without Battery Storage for Stand-Alone Applications”, International Conference on Electrical, Control and Computer Engineering, 2011, pp. 269 – 274.
- [4]. Miao Zhu, Fang Lin Luo, “Transient analysis of multi-state dc–dc converters using system energy characteristics”, International Journal of Circuit Theory and Applications 2008, vol.36, issue.3, pp. 327–344.
- [5]. William Chan, C. K. Tse, “Bifurcations in current-programmed DC/DC buck switching regulators—conjecturing a universal bifurcation path”, International Journal of Circuit Theory and Applications 1998, vol. 26, issue.2, pp.127–145.
- [6]. S. N. Bhadra, D. Kashta, S. Banerjee, “Wind Electrical System”, Oxford University Press 2005, chapter 7, page(s). 288 – 295.